

# [Ni(phen)<sub>3</sub>]<sub>2</sub>Sb<sub>18</sub>S<sub>29</sub>: A Novel Three-Dimensional Framework Thioantimonate(III) Templated by [Ni(phen)<sub>3</sub>] Complexes

Ke-Zhao Du,<sup>†,‡</sup> Mei-Ling Feng,<sup>†</sup> Long-Hua Li,<sup>†</sup> Bing Hu,<sup>†</sup> Zu-Ju Ma,<sup>†,‡</sup> Peng Wang,<sup>†,‡</sup> Jian-Rong Li,<sup>†</sup> Yu-Long Wang,<sup>†,‡</sup> Guo-Dong Zou,<sup>†,‡</sup> and Xiao-Ying Huang<sup>\*,†</sup>

<sup>†</sup>State Key Laboratory of Structural Chemistry, Fujian Institute of Research on the Structure of Matter, Chinese Academy of Sciences, Fuzhou, Fujian 350002, People's Republic of China

<sup>‡</sup>Graduate School of the Chinese Academy of Sciences, Beijing 100049, People's Republic of China

## S Supporting Information

**ABSTRACT:** A novel thioantimonate(III), namely, [Ni(phen)<sub>3</sub>]<sub>2</sub>Sb<sub>18</sub>S<sub>29</sub> (**1**; phen = 1,10-phenanthroline), has been solvothermally synthesized. Its structure features a three-dimensional framework with the largest channels in thioantimonates. The chiral [Ni(phen)<sub>3</sub>]<sup>2+</sup> cations and the Sb:S ratio (1:1.611) in **1** are unique among those in the reported thioantimonates. The thermal stability, optical properties, and electric conductivity as well as the theoretical band structure and density of state of **1** have also been studied.

Metal chalcogenides have attracted much attention in recent years owing to their potential applications in areas such as fast-ion conductivity,<sup>1</sup> ion exchange,<sup>2</sup> and tunable electronic and optical properties.<sup>3</sup> The research on thioantimonates(III) has been very fruitful in the past 2 decades because the stereochemical effect of the lone pair of electrons<sup>4</sup> and the wide range of coordination numbers of Sb<sup>III</sup> from 3 to 6 can lead to large structural and compositional diversities of thioantimonates(III).<sup>5</sup> Despite many thioantimonates(III) reported,<sup>4,6</sup> relatively little progress has been made on the preparation of the three-dimensional (3D) framework thioantimonates(III) when taking no account of the weaker secondary Sb–S interactions.<sup>7</sup> Thus far, only a few 3D thioantimonates have been reported, including K<sub>2</sub>Sb<sub>4</sub>S<sub>7</sub>,<sup>7a</sup> [Ni(aepa)<sub>2</sub>]<sub>2</sub>Sb<sub>4</sub>S<sub>7</sub>,<sup>7b</sup> [M(en)<sub>3</sub>]<sub>2</sub>[Sb<sub>12</sub>S<sub>19</sub>] (M = Co, Ni),<sup>7c,d</sup> [cyclamH<sub>2</sub>]<sub>2</sub>[Sb<sub>4</sub>S<sub>7</sub>],<sup>7e</sup> [Ni(cyclam)]<sub>2</sub>[Sb<sub>4</sub>S<sub>7</sub>],<sup>7e</sup> and [Co(cyclam)]<sub>x</sub>[cyclamH<sub>2</sub>]<sub>1-x</sub>[Sb<sub>4</sub>S<sub>7</sub>] (0.08 ≤ *x* ≤ 0.74).<sup>7e</sup>

On the other hand, usually 3D framework chalcogenides are constructed in the presence of organic amines or metal complexes as templates or structure-directing agents. It has been reported that metal (M)-phen/bpy (bpy = 2,2'-bipyridine) complexes are optically active species, and integration of such optically active species into the chalcogenide structures can improve the absorption band structure of the materials.<sup>8</sup> Some chalcogenides templated by M-phen/bpy complexes have been isolated.<sup>8,9</sup> However, thus far, there is no report on utilization of the M-phen complex as templates in the synthesis of chalcantimonate(III). Only several inorganic–organic hybrid manganese thioantimonate compounds were synthesized, in which the phen directly enters the thioantimonate moiety by chelation to the Mn<sup>II</sup> ion.<sup>10</sup> Here we report on the synthesis, crystal structure, and characterization of [Ni-

(phen)<sub>3</sub>]<sub>2</sub>Sb<sub>18</sub>S<sub>29</sub> (**1**), which represents the first polar 3D thioantimonate with the largest channels filled with two distinct arrays of [M(phen)<sub>3</sub>]<sup>2+</sup> complexes. Significantly, the first utilization of [M(phen)<sub>3</sub>]<sup>2+</sup> as templates and the Sb:S ratio (1:1.611) of **1** are unique among those in the reported thioantimonates.

Compound **1** was obtained from a mixture of Ni(CH<sub>3</sub>COO)<sub>2</sub>·4H<sub>2</sub>O, Sb<sub>2</sub>S<sub>3</sub>, S, and phen·H<sub>2</sub>O in a molar ratio of 1:1:3:1, 3 mL of ethanolamine, and 1 mL of H<sub>2</sub>O, which was sealed in a stainless steel reactor with a 20-mL Teflon liner and kept at 170 °C for 7 days. The product consisted of red clubbed crystals of **1** and a small amount of black powder. During synthesis, the templating cation was formed in situ.

Single-crystal X-ray crystallography reveals that **1** belongs to the polar space group P2<sub>1</sub>.<sup>11</sup> Its structure features a 3D framework with two-dimensional channels filled with the chiral [Ni(phen)<sub>3</sub>]<sup>2+</sup> cations. In the asymmetric unit of **1**, there are 18 crystallographically independent Sb atoms, 29 S atoms, and 2 [Ni(phen)<sub>3</sub>]<sup>2+</sup> complexes. Except for Sb1 and Sb2, the other 16 Sb atoms all are coordinated to 3 S atoms to form SbS<sub>3</sub> trigonal-pyramidal geometries, with the Sb–S distances ranging from 2.336(3) to 2.539(2) Å. Whereas both Sb1 and Sb2 are four-coordinated, with two short [2.423(2)–2.478(2) Å] and two long [2.616(2)–2.868(2) Å] Sb–S bonds, similar to those in the {Sb<sub>2</sub>S<sub>2</sub>} rings of the previously reported compound-<sub>s</sub>.<sup>6i,7c,d</sup>

As shown in Figure 1a, the Sb(9–16)S<sub>3</sub> trigonal pyramids are interconnected by sharing of the corners to form a {Sb<sub>8</sub>S<sub>8</sub>} ring (R1), whereas another similar {Sb<sub>8</sub>S<sub>8</sub>} ring (R2) consisting of Sb9, Sb(11–13), Sb(15–18), and eight S atoms is also observed that shares three SbS<sub>3</sub> units with R1. The alternating arrangements of the two types of {Sb<sub>8</sub>S<sub>8</sub>} rings result in a one-dimensional (1D) ribbon ([Sb<sub>10</sub>S<sub>18</sub>]<sub>n</sub><sup>6n-</sup>) along the *a* axis (Figure 1a). The Sb1S<sub>4</sub> and Sb2S<sub>4</sub> units share one edge (S4 and S6), forming a *trans*-[Sb<sub>2</sub>S<sub>6</sub>] dimer (Figure 1b). Interconnections of 1D ribbons of [Sb<sub>10</sub>S<sub>18</sub>]<sub>n</sub><sup>6n-</sup> by the tetradentate bridging [Sb<sub>2</sub>S<sub>6</sub>] dimers along the *c* axis lead to a [Sb<sub>12</sub>S<sub>20</sub>]<sub>n</sub><sup>4n-</sup> layer along the *ac* plane by sharing four S atoms (S2, S3, S7, and S10; Figure 1c). The new eight-membered {Sb<sub>8</sub>S<sub>8</sub>} rings (R3) are observed in the layer because of the [Sb<sub>2</sub>S<sub>6</sub>] dimers bridging 1D ribbons. In addition, two [Sb<sub>3</sub>S<sub>6</sub>]<sup>3-</sup> semicubes

Received: October 17, 2011

Published: March 22, 2012

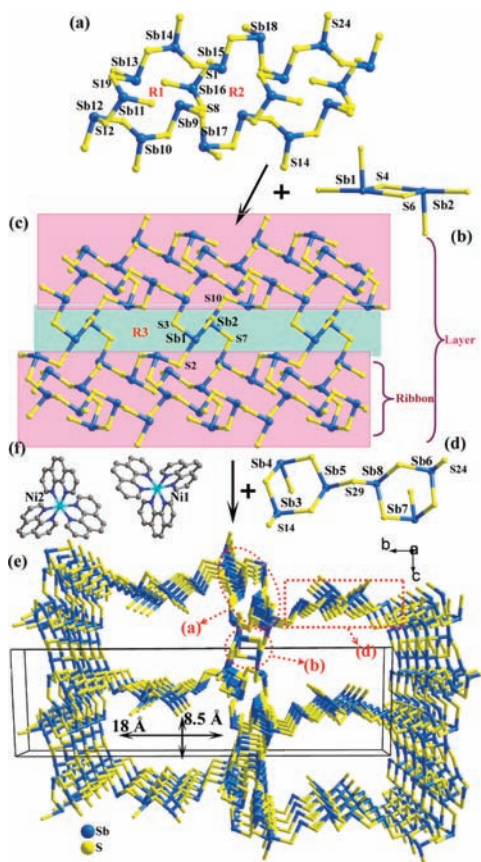


**Figure 1.** (a) 1D ribbon of  $[\text{Sb}_{10}\text{S}_{18}]_n^{4n-}$ . (b) *trans*- $[\text{Sb}_2\text{S}_6]$  dimer. (c)  $[\text{Sb}_{12}\text{S}_{20}]_n^{4n-}$  layer. (d)  $[\text{Sb}_6\text{S}_{11}]$  unit. (e) 3D framework of **1** viewed along the *a* axis. (f)  $[\text{Ni}(\text{phen})_3]^{2+}$  cations in the channel.

constructed of three  $\text{SbS}_3$  trigonal pyramids ( $\text{Sb}(3-5)\text{S}_3$  and  $\text{Sb}(6-8)\text{S}_3$ , respectively) are connected into a  $[\text{Sb}_6\text{S}_{11}]$  unit by sharing the S29 atom (Figure 1d). Then the  $[\text{Sb}_6\text{S}_{11}]$  units acting as linkers further cross-link the  $[\text{Sb}_{12}\text{S}_{20}]_n^{4n-}$  layers into a 3D  $[\text{Sb}_{18}\text{S}_{29}]_n^{4n-}$  anionic network (Figure 1e).

Viewed along the *a* axis, the 3D anionic network reveals large 1D channels consisting of 48-membered ring  $\{\text{Sb}_{24}\text{S}_{24}\}$  (Figure S1 in the Supporting Information, SI) with dimensions of approximately  $18 \times 8.5$  Å (Figure 1e). To the best of our knowledge, such 1D channels are the largest in the known 3D thioantimonates. The channels are occupied by two distinct arrays of  $[\text{Ni}(\text{phen})_3]^{2+}$  cationic complexes. It is worth noting that there is only one reported example of an open-framework chalcogenide featuring the  $[\text{Cd}_{32}\text{S}_{14}(\text{SC}_6\text{H}_5)_{38}]_n^{2n-}$  anionic network that is templated by M-phen complexes ( $[\text{Fe}(\text{phen})_3]^{2+}$  and  $[\text{Ru}(\text{phen})_3]^{2+}$ ).<sup>8f</sup> The two crystallographically distinct  $[\text{Ni}(\text{phen})_3]^{2+}$  complexes represent  $\Delta(\text{Ni}1)$  and  $\Lambda(\text{Ni}2)$  configurations (Figure 1f), respectively, which are similar to those in  $[\text{Co}(\text{en})_3][\text{Sb}_{12}\text{S}_{19}]^{7d}$  and  $[\text{M}(\text{dap})_3]\text{InSb}_3\text{S}_7$  ( $\text{M} = \text{Co}, \text{Ni}$ ).<sup>12</sup> Moreover, another type of channel ( $15.6 \times 9.5$  Å) with a narrow waist is found along the *c* axis (Figure S2 in the SI). From the topological point of view, the 3D network of **1** is  $\text{pcu}$  ( $4^{12}\cdot 6^3$ ) topology built upon a six-connected net (Figure S4 in the SI). Furthermore, the  $[\text{Ni}(\text{phen})_3]^{2+}$  complexes form weak C–H $\cdots$ S hydrogen bonds with the S atoms of the 3D anionic network (Figure S3 in the SI).

The optical absorption spectrum (Figure 2) of compound **1** indicates a sharp absorption edge at about 2.16 eV, which is consistent with its red color. There is a noticeable red shift of

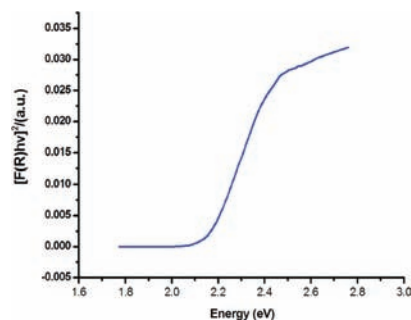


**Figure 2.** Solid-state optical absorption spectrum of **1**.

the absorption edge of **1** compared with that in the known low-dimensional thioantimonates containing metal complexes, such as  $[\text{Ni}(\text{dap})_3]\text{Sb}_4\text{S}_7$  (2.44 eV),<sup>6b</sup>  $[\text{Ni}(\text{en})_3]\text{Sb}_2\text{S}_4$  (2.49 eV),<sup>6f</sup> and  $[\text{Ni}(\text{en})_3]\text{Sb}_4\text{S}_7$  (2.62 eV).<sup>6f</sup>

To further investigate the electronic structure of **1**, the band structure and density of state (DOS) calculations for **1** have been studied. The methodology used for the band structure calculations is described in the SI. Compound **1** has a direct band gap of around 1.12 eV, which is significantly smaller than the experimental value (2.16 eV). As is well-known, the generalized gradient approximation does not accurately describe the eigenvalues of the electronic states, which often causes quantitative underestimation of the band gaps for semiconductors and insulators.<sup>13</sup> In the DOS curve (Figure S5 in the SI), the conduction bands in the energy range of 0–1.5 eV above the Fermi level (the Fermi level is set at 0.0 eV) are mainly contributed by Ni 3d, C 2p, and N 2p states, and the states (1.5–4.5 eV) are dominated by Sb 5p, S 3p, C 2p, and N 2p, while the valence bands from –1.5 eV to the Fermi level are derived from Sb 5p and S 3p. Therefore, the band gap of compound **1** is primarily the result of the charge-transfer transition from the anion  $[\text{Sb}_{18}\text{S}_{29}]^{4-}$  to the cation  $[\text{Ni}(\text{phen})_3]^{2+}$ . This is similar to that previously reported for sulfides containing transition-metal-phen (or bipy) complexes,<sup>8d,e</sup> but it is quite different from the observation that the optical band gap of antimony sulfides depends more on the density of the anionic framework (measured by the number of Sb metal atoms per 1000 Å).<sup>6a</sup> To further understand the origin of the optical band gap, we also did theoretical band structure and DOS calculations of  $[\text{Ni}(\text{dien})_2]\text{Sb}_6\text{S}_{10}$ <sup>6c</sup> for comparison, which possesses a framework density and a band gap similar to those of **1**. The results (Figures S7 and S8 in the SI) show that the band gap of  $[\text{Ni}(\text{dien})_2]\text{Sb}_6\text{S}_{10}$  mainly depends on the states of the atoms in the anionic framework, while C, N, and H contribute little, in contrast to that in the title compound. Clearly, M-phen in **1** as an optically active species can tune the optical absorption of the material.

The room-temperature resistance for **1** is 39.36 kΩ (Figure 3). When the dimensions are taken into account, the electrical conductivity is  $2.9 \times 10^{-3}$  S·cm<sup>-1</sup>.

Simultaneous thermogravimetric analysis (TGA–DSC; Figure S10 in the SI) from 30 to 460 °C on the powder (7.669 mg) of compound **1** indicated that it was stable up to 280 °C and then decomposed in one step with a total weight loss of 23.69%, which was mostly attributed to the removal of six phen molecules per formula (theoretical weight loss of 25.03%). Interestingly, when **1** was heated up to 850 °C, hexagonal NiSb, which is a potential Li-ion battery anode material and is technologically important in secondary high-

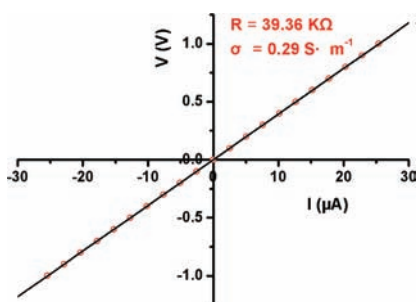


Figure 3. Room-temperature conductivity for **1**.

temperature batteries,<sup>14</sup> could be identified in the powder X-ray diffraction pattern of the residues (Figure S12 in the SI).

In summary, we have presented solvothermal synthesis, crystal structure, thermal stability, optical and electric conductivity, and theoretical calculations of a polar 3D (neglecting secondary Sb–S interactions) thioantimonate **1** with the largest channels, a unique Sb:S ratio (1:1.611), and metal-phen-templating cations. The results of the calculations indicate that the band gap of compound **1** is likely determined by the conduction band edge of cations and the valence band edge of anions. Further studies will focus on the synthesis and structure–property relationship of 3D chalcantimonates templated by various M-phen (or bipy, M = transition-metal ions).

## ■ ASSOCIATED CONTENT

### ■ Supporting Information

Crystallographic data in CIF format, table of hydrogen-bond data, calculated band structure, elemental analysis, IR, TGA, and powder X-ray diffraction patterns. This material is available free of charge via the Internet at <http://pubs.acs.org>.

## ■ AUTHOR INFORMATION

### ■ Corresponding Author

\*E-mail: xyhuang@fjirsm.ac.cn.

## ■ ACKNOWLEDGMENTS

This work was supported by the Knowledge Innovation Program of the Chinese Academy of Sciences (Grant KJCX2-YW-H21), the NNSF of China (Grants 20873149 and 20803081), and the NSF of Fujian Province (Grants 2008J0174 and 2010J01056).

## ■ REFERENCES

- (1) Zheng, N.; Bu, X.; Feng, P. *Nature* **2003**, *426*, 428–432.
- (2) (a) Li, J.-R.; Huang, X.-Y. *Dalton Trans.* **2011**, *40*, 4387–4390. (b) Feng, M.-L.; Kong, D.-N.; Xie, Z.-L.; Huang, X.-Y. *Angew. Chem., Int. Ed.* **2008**, *47*, 8623–8626.
- (3) Zheng, N.; Bu, X.; Wang, B.; Feng, P. *Science* **2002**, *298*, 2366–2369.
- (4) Parise, J. B. *Science* **1991**, *251*, 293–294.
- (5) (a) Zhou, J.; Dai, J.; Bian, G.-Q.; Li, C.-Y. *Coord. Chem. Rev.* **2009**, *253*, 1221–1247. (b) Sheldrick, W. S.; Wachhold, M. *Coord. Chem. Rev.* **1998**, *176*, 211–322.
- (6) (a) Powell, A. V.; Lees, R. J. E.; Chippindale, A. M. *J. Phys. Chem. Solids* **2008**, *69*, 1000–1006. (b) Zhou, J.; Bian, G.-Q.; Zhang, Y.; Dai, J.; Cheng, N. *Z. Anorg. Allg. Chem.* **2007**, *633*, 2701–2705. (c) Lees, R. J. E.; Powell, A. V.; Chippindale, A. M. *J. Phys. Chem. Solids* **2007**, *68*, 1215–1219. (d) Schaefer, M.; Kurowski, D.; Pfitzner, A.; Nather, C.; Rejai, Z.; Moller, K.; Ziegler, N.; Bensch, W. *Inorg. Chem.* **2006**, *45*, 3726–3731. (e) Schaefer, M.; Nather, C.; Lehnert, N.; Bensch, W.

*Inorg. Chem.* **2004**, *43*, 2914–2921. (f) Stephan, H.-O.; Kanatzidis, M. G. *Inorg. Chem.* **1997**, *36*, 6050–6057. (g) Ko, Y. H.; Tan, K. M.; Parise, J. B.; Darovsky, A. *Chem. Mater.* **1996**, *8*, 493–496. (h) Parise, J. B.; Ko, Y. H. *Chem. Mater.* **1992**, *4*, 1446–1450. (i) Volk, K.; Bickert, P.; Kolmer, R.; Schafer, H. Z. *Naturforsch. B* **1979**, *34*, 380–382.

(7) (a) Graf, H. A.; Schafer, H. Z. *Naturforsch. B* **1972**, *27b*, 735. (b) Seidlhofer, B.; Djamil, J.; Näther, C.; Bensch, W. *Cryst. Growth Des.* **2011**, *11*, 5554–5560. (c) Lees, R. J. E.; Powell, A. V.; Chippindale, A. M. *J. Phys. Chem. Solids* **2007**, *68*, 1215–1219. (d) Vaqueiro, P.; Chippindale, A. M.; Powell, A. V. *Inorg. Chem.* **2004**, *43*, 7963–7965. (e) Powell, A. V.; Lees, R. J. E.; Chippindale, A. M. *Inorg. Chem.* **2006**, *45*, 4261–4267.

(8) (a) Zhang, Y.-P.; Zhang, X.; Mu, W.-Q.; Luo, W.; Bian, G.-Q.; Zhu, Q.-Y.; Dai, J. *Dalton Trans.* **2011**, *40*, 9746–9751. (b) Zhang, X.; Luo, W.; Zhang, Y.-P.; Jiang, J.-B.; Zhu, Q.-Y.; Dai, J. *Inorg. Chem.* **2011**, *50*, 6972–6978. (c) Zhao, J.; Liang, J.-L.; Chen, J.-F.; Pan, Y.-L.; Zhang, Y.; Jia, D.-X. *Inorg. Chem.* **2011**, *50*, 2288–2293. (d) Jiang, J.-B.; Bian, G.-Q.; Zhang, Y.-P.; Luo, W.; Zhu, Q.-Y.; Dai, J. *Dalton Trans.* **2011**, *40*, 9551–9556. (e) Liu, G.-N.; Guo, G.-C.; Chen, F.; Guo, S.-P.; Jiang, X.-M.; Yang, C.; Wang, M.-S.; Wu, M.-F.; Huang, J.-S. *CrystEngComm* **2010**, *12*, 4035–4037. (f) Zheng, N.-F.; Lu, H.-W.; Bu, X.-H.; Feng, P.-Y. *J. Am. Chem. Soc.* **2006**, *128*, 4528–4529.

(9) (a) Jia, D.; Zhao, J.; Pan, Y.; Tang, W.; Wu, B.; Zhang, Y. *Inorg. Chem.* **2011**, *50*, 7195–7201. (b) Lei, Z.-X.; Zhu, Q.-Y.; Zhang, X.; Luo, W.; Mu, W.-Q.; Dai, J. *Inorg. Chem.* **2010**, *49*, 4385–4387.

(10) (a) Lin, Z.-E.; Bu, X.-H.; Feng, P.-Y. *Microporous Mesoporous Mater.* **2010**, *132*, 328–334. (b) Wang, X.; Sheng, T.-L.; Hu, S.-M.; Fu, R.-B.; Wu, X.-T. *Inorg. Chem. Commun.* **2009**, *12*, 399–401.

(11) Crystal data for **1**: C<sub>72</sub>H<sub>48</sub>N<sub>12</sub>Ni<sub>2</sub>S<sub>29</sub>Sb<sub>18</sub>, M = 4319.88, monoclinic, P2<sub>1</sub>, a = 11.17374(16) Å, b = 41.2997(5) Å, c = 12.37007(19) Å, β = 106.5568(15)°, V = 5471.76(14) Å<sup>3</sup>, Z = 2, D<sub>calc</sub> = 2.662 g·cm<sup>-3</sup>, F(000) = 4004, μ = 5.293 mm<sup>-1</sup>, T = 293(2) K, 25504 reflections measured, 17271 unique reflections (R<sub>int</sub> = 0.023), 16490 observed reflections [I > 2σ(I)] with RI (wR2) = 0.0304 (0.0716), RI (wR2) = 0.0326 (0.0729) (all data), GOF = 1.024. CCDC 847909.

(12) Zhou, J.; An, L.; Zhang, F. *Inorg. Chem.* **2011**, *50*, 415–417.

(13) (a) Terki, R.; Bertrand, G.; Aourag, H. *Microelectron. Eng.* **2005**, *81*, 514–523. (b) Okoye, C. M. I. *J. Phys. Condens. Mater.* **2003**, *15*, 5945–5958. (c) Godby, R. W.; Schluter, M.; Sham, L. J. *Phys. Rev. B* **1987**, *36*, 6497–6500.

(14) (a) Kumari, L.; Li, W.-Z.; Huang, J.-Y.; Provencio, P. P. *J. Phys. Chem. C* **2010**, *114*, 9573–9579. (b) Xie, J.; Zhao, X.-B.; Yu, H.-M.; Qi, H.; Cao, G.-S.; Tu, J.-P. *J. Alloys Compd.* **2007**, *441*, 231–235.